Modification of Silver Oxide/Silver Doped Titanium Dioxide ($Ag_2O/Ag\text{-}TiO_2$) Photocatalyst Using an Immobilized Reverse Photodeposition Method for Photodegradation of Reactive Red 4 Dye

Nur Syamimi Adzis, Nur Hidayatul Syazwani Suhaimi, Nureel Imanina Abdul Ghani, Nur Fatin Najihah Abd Yami, Nur Aein Muhamad, Muhammad Saifulddin Mohd Azami[1] and Wan Izhan Nawawi*

Faculty of Applied Sciences, Universiti Teknologi MARA, 02600 Arau, Perlis, Malaysia
*Corresponding author (e-mail: wi_nawawi@uitm.edu.my)

A new immobilized Z-scheme heterojunction of Ag_2O/Ag doped TiO_2 using a reverse technique to prevent excess chemical usage was prepared by immobilizing TiO_2 prior to doping with silver and silver oxide nanoparticles by a photodeposition method using a 250-Watt fluorescent lamp irradiation process for 60 min. TiO_2 was coated onto double-sided adhesive tape (DSAT) using the brush technique, and a glass plate measuring 10 x 1.5 x 0.2 cm (L x H x B) was used as the support material for immobilization. Reactive Red 4 (RR4) dye was used as a model pollutant to measure the photocatalytic activity of the prepared immobilized $Ag_2O/Ag\text{-}TiO_2$. Characterization was performed by X-ray diffraction, photoluminescence, UV-vis diffuse reflectance spectroscopy and FESEM equipped with energy dispersive X-ray analysis (EDX). The results showed that Z-scheme heterojunctions of $Ag_2O/Ag\text{-}TiO_2$ significantly enhanced photocatalytic degradation compared to the N-type TiO_2 microsphere. In comparison with pure TiO_2, the modified composite photocatalyst exhibited higher photocatalytic activity under visible light irradiation in the decomposition of RR4 in aqueous solution. The photocatalytic degradation followed the pseudo-first-order reaction model. The heterostructure with a 3 % molar ratio of TiO_2 and $AgNO_3$ exhibited the best photocatalytic activity with an apparent first-order rate constant of 0.321 min^{-1}.

Keywords: Immobilized TiO_2; reversed photodeposition; DSAT immobilization; photocatalytic degradation; silver oxide

Received: May 2023; Accepted: July 2023

With the growth of the industrial sector, the amount of wastewater generated as a by-product has also increased. Physical separation, for example, cannot be used for wastewater from the textile industry because it contains hydrophilic organic compounds. Without appropriate treatment, these organic compounds are discharged into water bodies (Kouhail et al., 2020). Wastewater from the textile industry includes a high concentration of toxic recalcitrant colouring pollutants, dissolved solids and toxic materials that can persist in the environment for long periods of time (Kishor et al., 2021). Moreover, reactive dyes in organic wastewater make water remediation more challenging. There are several chemical approaches for wastewater treatment. However, photocatalysis has garnered considerable attention from researchers as it offers low-cost treatment, complete degradation, and eco-friendliness. Photocatalysis is a potential treatment method that can degrade organic pollutants (dyes) using a redox reaction technique (Kouhail et al., 2020). In this process, organic pollutants are oxidized and reduced simultaneously, transforming them into carbon dioxide (CO_2) and water (H_2O). Titanium dioxide (TiO_2), zinc oxide (ZnO), ferric oxide (Fe_2O_3) and other semiconductor materials work as photocatalysts for various applications (Gilja et al., 2018). TiO_2 is one of the most commonly used photocatalyst materials (Gomes et al., 2018; Komaraiah et al., 2020; Arekhi & Jamshidi, 2018). It is known for its non-toxic behaviour, low cost, and sturdy applicability for the photocatalytic degradation (PCD) of organic pollutants. It is important to emphasize that TiO_2 is an n-type semiconductor with a high energy band gap (E_g) of 3.2 eV. However, the photocatalytic activity of TiO_2 is limited due to the high band gap energy, high recombination of the photogenerated electron-hole pair (e^-/h^+), wide electron trapping and lack of surface-active sites (Varma et al., 2020). Thus, modification of TiO_2 is crucial to create a more stable charge carrier separation and electron movement that can enhance its photocatalytic performance. Many attempts have been made to improve the photocatalytic efficacy of mesoporous TiO_2 by decorating the surface with metals (Ag, Pt, Pd) and non-metals (C, N, P). However, although the visible light absorption can be improved, TiO_2's efficacy as an oxidation photocatalyst is still relatively low. Hence, combining TiO_2 with another

semiconductor is a viable alternative to provide a new route of charge transfer through the junction created between both semiconductors. A heterojunction system can not only improve charge carrier transfer but has also been widely applied to expedite the degradation process and enhance the photoefficiency for the oxidation of dyes under moderate light energy. Recently, the metal oxide Ag_2O, which has a narrow band gap (Eg = 1.0-1.46 eV) and a known stability, was found to match well with TiO_2 due to their band gap structures. Together, they created a p-n hetero-junction system, that resulted in enhanced light absorption and accumulation of photogenerated e^-/h^+ pairs separation. This was demonstrated by the high stability of the Ag_2O/TiO_2 system in the photo-destruction of dyes under visible light illumination, which was linked to the participation of $Ag_2O–TiO_2$ surface p-n junctions that facilitated electron transfer between semiconductors, as shown in Figure 1.

Recently, the use of $Ag_2O\text{-}TiO_2$ suspensions has become the standard approach for wastewater remediation due to its high surface-to-volume ratio (Razak et al., 2014). However, this results in the treated wastewater being in a slurry form, requiring a filtration process. As a result, $Ag_2O\text{-}TiO_2$ cannot be reused, making it impractical for commercial applications. TiO_2 immobilization was introduced to eliminate the post-treatment filtration process and make TiO_2 reusable. Previously, the conventional method used self-sedimentation, in which the treatment required the use of alum (aluminium sulphate) as the coagulant (Jagaba et al., 2018). This was not practical as it required many post-treatment steps and had a very high cost due to the chemicals used. Moreover, these may also produce harmful by-products.

TiO_2 immobilization involves applying a photo-catalyst onto a solid support material to hold them together (Ismail et al., 2015). Some researchers have used polymer binders due to their strong adhesion with immobilized TiO_2. However, an excessive amount of polymer has the drawback of reducing the contact surface of TiO_2 with pollutants (Ismail et al., 2015). Hence, the TiO_2 immobilization technique is more favourable as it eliminates the need for post-treatment filtration. However, the use of immobilized TiO_2 is still not practical due to interference from excessive polymer binders.

Double-sided adhesive tape (DSAT) has been introduced as the most effective alternative to polymer matrix binders in the TiO_2 immobilization system. DSAT shows great potential for replacing polymer binders in the immobilization system. It possesses good characteristics such as being waterproof, long-lasting, and having strong adhesion with various materials (Ismail et al., 2015). The typical preparation technique for immobilized TiO_2 involves modifying $Ag_2O\text{-}TiO_2$ in a slurry form using TiO_2 powder and then coating it using the immobilization technique, typically brushing. Immobilized $Ag_2O\text{-}TiO_2$ has shown better photocatalytic activity compared to immobilized unmodified TiO_2 using the conventional technique. Immobilized $Ag_2O\text{-}TiO_2$ is commonly prepared via photodeposition prior to immobilization. However, a few studies have reported that the interaction of the prepared $Ag_2O\text{-}TiO_2$ powder with solvents during the immobilization process reduces its photocatalytic performance. Hence, avoiding solvent usage during immobilization is vital to minimize chemical interactions. Therefore, using the DSAT technique prior to doping with Ag_2O is the best method for preparing immobilized $Ag_2O\text{-}TiO_2$.

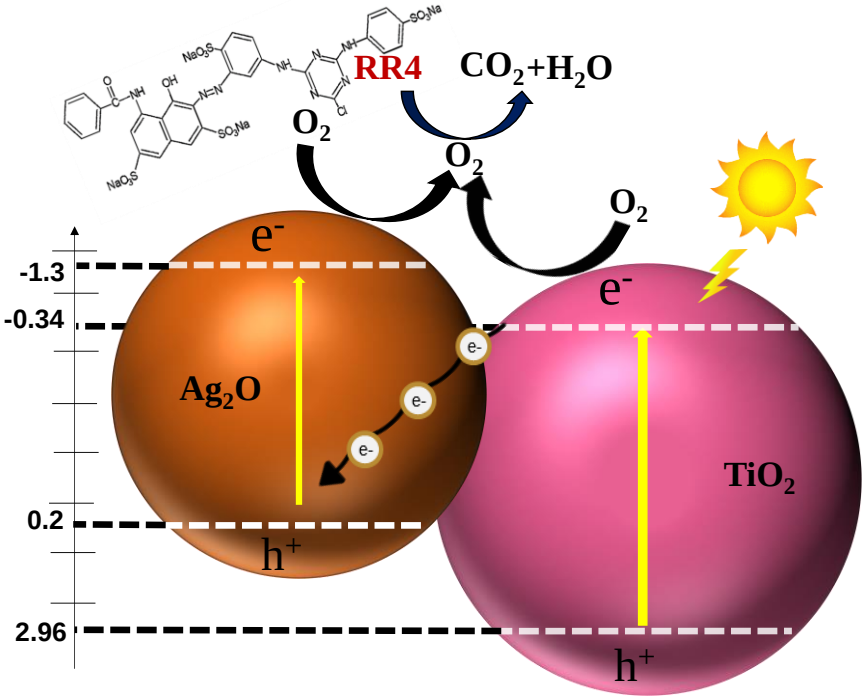

Figure 1. Proposed mechanism of p-n heterojunction of $Ag_2O\text{-}TiO_2$.

EXPERIMENTAL

Chemicals and Materials

TiO_2 powder (Degussa P25, 20% rutile, 80% anatase) was supplied by Merck, distilled/deionized water was used as the solvent for all experiments, Reactive Red-4 dye powder, purchased from Sigma-Aldrich, was used as a model pollutant. Polyvinyl alcohol (PVA) provided by R&M was used as a matrix adding solution, and silver nitrate from QRec ($AgNO_3$) was used as a Ag precursor.

A glass plate measuring 10 x 1.5 x 0.2 cm (L x H x B) was used as a support material for TiO_2 immobilization. A 55-Watt fluorescent lamp model Firefly/E27 was used during the irradiation process. A 250 mL Schott bottle was used to store the TiO_2 formulation. Double sided Adhesion Tape (DSAT) from Newstar was used as the main binder to hold the TiO_2 nanoparticles. A multifunctional orbital shaker from Grant-bio was used to shake the formulation.

Preparation of Immobilized TiO_2

About 6.5 g of TiO_2 powder (P25, Degussa, 80% anatase and 20% rutile) was added to 40 mL of distilled water in a 250 mL reagent bottle and stirred for a few seconds. Then, about 1 ml of PVA (8%) was added, and the TiO_2 mixture was put through a shaking process for 5 minutes to make sure it was in the form of a homogenized white solution. After that, DSAT was taped on the glass plate and a brush coating technique was used to coat the prepared TiO_2 formulation on the taped surface. The glass plate coated with 0.1 g of the TiO_2 formulation was dried under a hot air blower for 60 seconds at ± 80 °C. The dried immobilized TiO_2 was then cleaned with distilled water under irradiation with the fluorescent lamp, at 6400 K in aerated conditions for 60 minutes. The process was performed for 1 h prior to the silver doping process using the reverse method and photo-catalytic degradation study.

Preparation of Immobilized $Ag/Ag_2O\text{-}TiO_2$

Immobilized Ag_2O/Ag doped TiO_2 was synthesized using a reverse method. Solutions containing 1 wt%, 2 wt%, 3 wt% and 4 wt% of Ag were prepared using silver nitrate ($AgNO_3$) as a Ag precursor to dope the immobilized TiO_2. The reverse photodeposition method was carried out by pouring about 80 ml of a solution of aqueous $AgNO_3$ in 50% of IPA into a Schlenk tube. The glass plate coated with immobilized TiO_2 was hung by a thread and immersed in the solution. Then, the Schlenk tube was placed under vacuum for 10 seconds followed by purging with N_2 gas for 10 seconds. This step was repeated three times. After that, the immobilized TiO_2 and $AgNO_3$ aqueous solution was irradiated with a 250-Watt metal halide lamp for about 1 h to form immobilized $Ag_2O\text{-}TiO_2$.

Characterization Methods

An X-ray diffractometer (RIGAKU/XRD D/MAX 2200V/PC) with Cu Kα radiation at a wavelength of 1.5418 Å at 50 kV and a diffraction angle range of 2θ from 20°- 80° with a Lynx Eye detector was used to study the crystalline nature, phases and crystal sizes in the unmodified immobilized TiO_2 and immobilized $Ag_2O/Ag\text{-}TiO_2$ (Mogal et al., 2014; Estephane & El Jamal, 2019). A Hitachi SU8020 FESEM instrument equipped with Energy Dispersive X-Ray analysis (EDX) was utilized primarily to determine the surface morphology of the unmodified immobilized TiO_2 and immobilized $Ag_2O/Ag\text{-}TiO_2$ particles and the dispersion of metals on the catalyst surface (Mogal et al., 2014). The EDX analysis was performed randomly at points selected from the SEM analysis. About 20 kV of accelerating potential was used during the analysis. High-resolution TEM (HRTEM) images of the samples were taken by a JEOL-2100 instrument operated at an accelerating voltage of 200 kV. The samples were characterized with a Fourier Transform Infrared – Attenuated Total Reflectance (FTIR – ATR) instrument (Perkin-Elmer, model system 2000 FTIR) to determine the functional group or bonds in TiO_2 and $Ag_2O/Ag\text{-}TiO_2$ (1wt%, 2 wt%, 3 wt%, 4%). The absorbance from the photocatalytic degradation of RR4 was analysed by UV – Vis spectroscopy at 517 nm. Photoluminescence (PL) analysis was carried out using a Cary Eclipse Fluorescence Spectrophotometer with a xenon lamp. The UV-vis diffuse reflectance spectra were recorded using a UV-vis-near-infrared (NIR) spectrophotometer (Agilent, Cary 5000) in the range of 200-800 nm.

Photocatalytic Degradation of $Ag/Ag_2O\text{-}TiO_2$

About 12 ml of a 30 ppm solution of the anionic RR4 dye was poured into a custom glass cell with dimensions of 2 cm x 8 cm x 1.2 cm (L x H x B). The prepared immobilized $Ag_2O\text{-}TiO_2$ was then immersed in this solution. The solution was radiated with the fluorescent lamp for 15 min until the dye solution turned completely colourless. An aerator source, an aquarium pump model NS 7200, was used to supply oxygen for the reaction at 15 mL/min. A HACH DR 1900 spectrometer was used to determine the percentage of decolourization of RR4 from the photo-degradation process at a wavelength of 517 nm. A graph of these values against irradiation or contact time was plotted to determine the k value and linear correlation value. The results were converted into ln Co/C where Co was the absorbance of the initial concentration and C was the absorbance at any time (t). Based on the Langmuir-Hinshelwood rate model, the slope of the line was taken as the pseudo first order rate constant.

$$\text{Degradation rate (\%)} = \frac{C}{C_O} \times 100\%$$

Where C_O is the initial concentration and C is the final concentration.

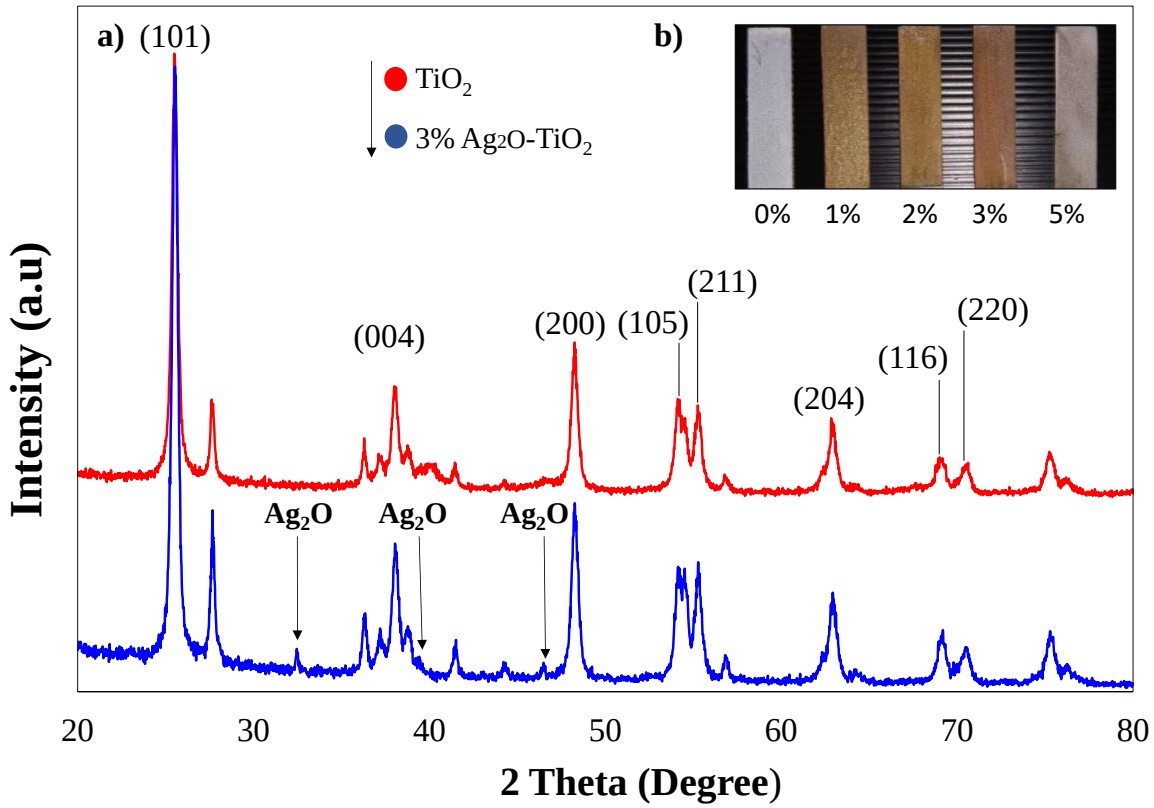

Figure 2. XRD spectrum of (a) Unmodified TiO_2 and modified 3% Ag_2O-TiO_2, (b) Physical color of 1-5% of Ag_2O-TiO_2.

RESULTS AND DISCUSSION

Characterization Study

The crystalline nature of the phases present in the unmodified TiO_2 and modified Ag_2O-TiO_2 was studied by X-ray diffraction (XRD). The X-ray diffractograms of the photocatalysts are shown in Figure 2. The XRD patterns of both unmodified TiO_2 and Ag_2O-TiO_2 were comparable to JCPDS File No: 894921. Based on the results, the XRD pattern of pure TiO_2 was consistent with that of anatase, exhibiting strong diffraction peaks at (101), (004), (200), (105), (211), (204), (116) and (220) which were assigned to diffraction angles (2θ) of 25.4°, 37.8°, 48.2°, 54.0°, 55.1°, 62.7°, 69.0° and 70.5°, respectively (JCPDS No. 21-1272).

The XRD analysis did not identify any peaks indicating a phase transformation from anatase to rutile. This may be attributed to the fact that the process was carried out under low heat, below 600 °C. In the spectra of 3 % Ag_2O-TiO_2, additional peaks appeared at the (110) and (200) planes with diffraction angles of 32.5°, 39.6° and 46.5°, indicating the presence of Ag_2O (JCPDS No. 4-0783) (Rozina et al., 2022; Oje et al., 2021). The cubic phase of Ag_2O was found in the Bragg peaks of the (200) crystal plane (ICDD CARD number: 041-1104) (Oje et al., 2021). The intensity of the detected Ag_2O was low due to the low loading of the $AgNO_3$ precursor. Furthermore, the small amount of Ag used in the doping process relative to the amount of TiO_2 on the plate resulted in no additional peaks from Ag, likely due to the high dispersion of Ag particles on the surface of TiO_2 (Komaraiah et al., 2020). It should be noted that an increase in the concentration of the loading precursor would result in a higher intensity of the peak. Therefore, XRD analysis confirmed that Ag_2O was incorporated into TiO_2. During the process, oxidation occurred, and silver nitrate was oxidized to silver oxide (Ag_2O) during photodeposition. The reaction mechanism of Ag_2O can be seen in Equations 1 and 2. The oxygen molecules in TiO_2 may have also contributed to the oxidation of Ag to Ag_2O. However, there was no indication of Ag doping with TiO_2 in the XRD results.

$$Ag^+ + OH^- \rightarrow AgOH \quad (1)$$

$$2AgOH \rightarrow Ag_2O + H_2O \quad (2)$$

Field emission scanning electron microscopy (FESEM) coupled with energy-dispersive X-ray spectroscopy (EDX) was used to characterize the morphology changes in TiO_2 after doping with silver oxide. Figures 3(a-b) and 3(c-d) depict the FESEM-EDX images of unmodified TiO_2 and 3 % Ag_2O-TiO_2,

respectively. The morphological features of TiO_2 were almost unchanged after being modified by Ag_2O, with spherical contours of nanoparticles clumping together and some small agglomerations forming microstructures. Based on Figures 3(a) and 3(c), it can be observed that 3 % Ag_2O-TiO_2 had a darker colour and numerous dark spots compared to TiO_2. This could indicate Ag or Ag_2O deposition on the surface of TiO_2.

However, due to the small particle size of unmodified TiO_2 and Ag_2O-doped TiO_2, the SEM resolution was inadequate to prove the deposition of Ag_2O and TiO_2 particles (Komaraiah et al., 2020). Therefore, elemental analysis (EDX) was used to identify the composition of materials present in unmodified TiO_2 and 3 % Ag_2O-TiO_2, as shown in Figures 3(b) and 3(d), respectively. The EDX pattern of unmodified TiO_2 showed peaks corresponding to the Ti and O components, while in the case of 3 % Ag_2O-TiO_2, there was a weak peak corresponding to the Ag component along with the Ti and O components. The weight percent (wt %) of Ag detected in the 3 % Ag_2O-TiO_2 was 0.6 %, as shown in Table 1. The presence of Ag and Ag_2O on the surface of TiO_2 implied a successful synthesis, as the EDX data confirmed the simultaneous deposition of Ag^0 and Ag_2O.

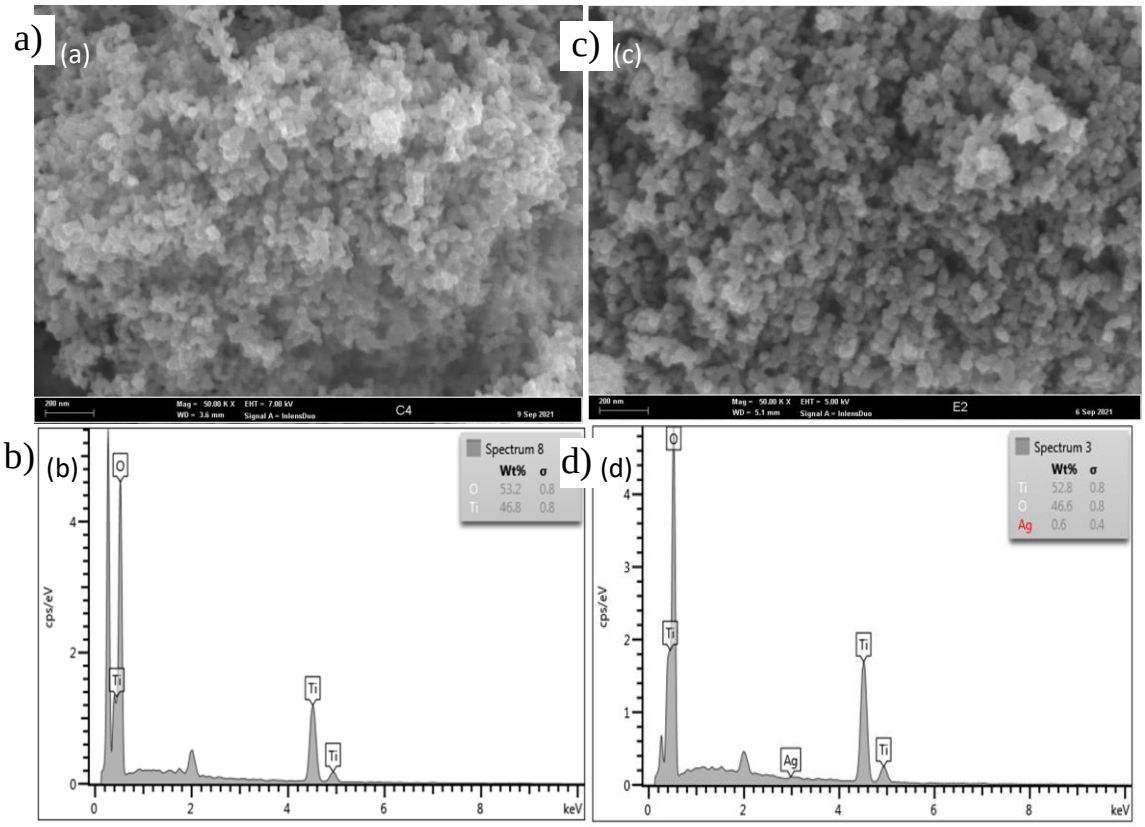

Figure 3. FESEM and EDX images of (a)-(b) – unmodified TiO_2 and (c)-(d) – modified 3% Ag_2O-TiO_2.

Table 1. Elemental analysis of synthesized nanocomposite.

Element	Weight (%)	Atomic (σ)
O	46.6	0.8
Ti	52.8	0.8
Ag	0.6	0.4
Total	100.0	

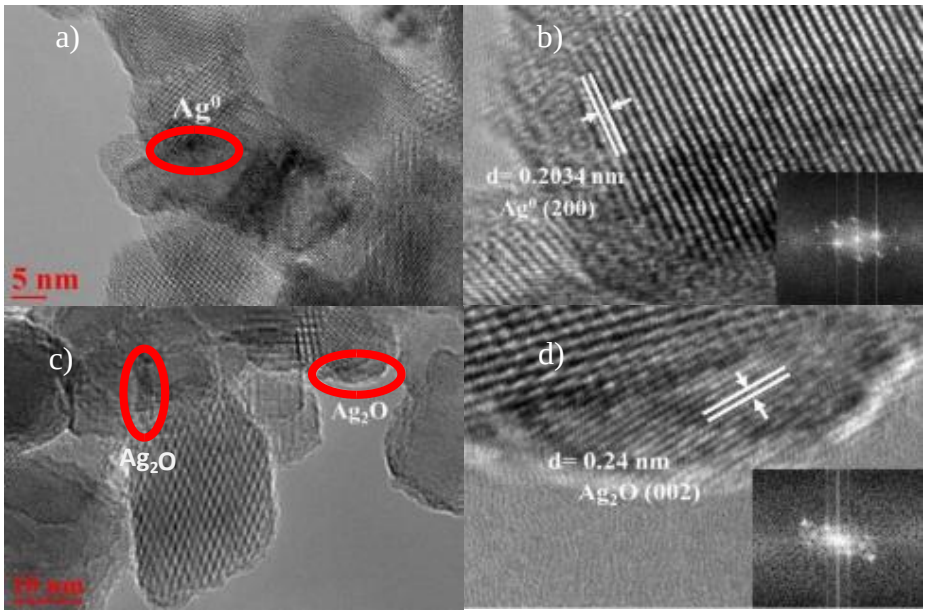

Figure 4. HRTEM images showing the presence of (a) metallic silver Ag^0, (b) d-spacing of Ag^0, (c) silver oxide, Ag_2O and (d) d-spacing of Ag_2O on TiO_2.

High-resolution transmission electron microscopy (HRTEM) was employed to examine the morphology of synthetic pure TiO_2 and the Ag/Ag_2O-TiO_2 heterojunction, with 3% silver loading. Figure 4 illustrates the HRTEM images, revealing the internal morphological features of the Ag/Ag_2O-TiO_2 photocatalyst had various shapes, including spherical, cubic, and hexagonal. Overall, the images clearly show numerous dark spots on the TiO_2 surface, indicating the presence of Ag_2O or Ag nanoparticles. In Figure 4(c), the appearance of Ag_2O nanoparticles on the TiO_2 surface can be observed, and in Figure 4(d), the HRTEM micrograph demonstrates the composite material formed by Ag_2O, indexed as (002) with a spacing of d = 0.24 nm. Additionally, Figure 4(a) shows the presence of Ag nanoparticles, suggesting that Ag^0 may contribute to the photocatalytic performance/efficacy of this sample by acting as a dopant that exhibits localized surface plasmon resonance (LSPR) during electronic accumulation, thereby helping to reduce the charge recombination problem. Figure 4(b) displays the deposition of Ag^0 on TiO_2, as detected by the spacing of d = 0.2034 nm indexed at (200). Thus, the HRTEM images confirm the presence of both Ag_2O and Ag^0 on TiO_2, which is consistent with the SEM and XRD results.

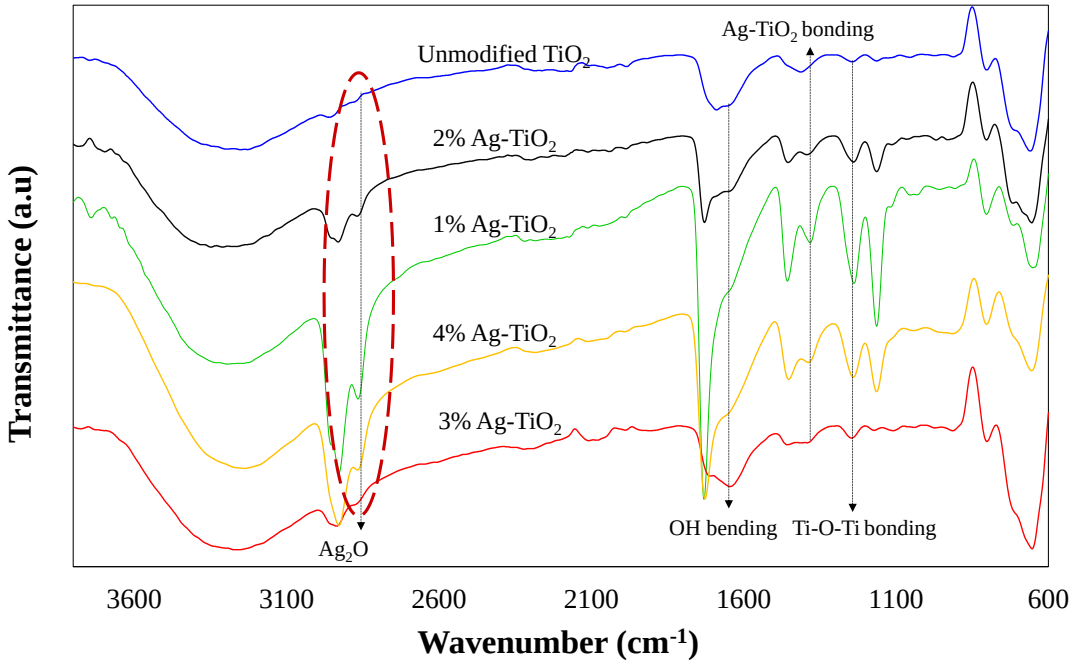

Figure 5. FTIR spectra of unmodified TiO_2 and modified Ag-TiO_2.

Next, Figure 5 shows the FTIR spectra for the unmodified and modified $Ag_2O\text{-}TiO_2$ doped TiO_2 photocatalysts. It was observed that all samples exhibited broad peaks between 3000-3400 cm^{-1} that centred around 3262 cm^{-1}, corresponding to the stretching vibration of the hydroxyl group (-OH), and at 1651 cm^{-1}, corresponding to –OH bending (Govindan & Soliman, 2017). The number of hydroxyl groups in $Ag_2O\text{-}TiO_2$ determines its photocatalytic activity. More -OH functional groups contribute to an increased production of hydroxyl radicals, which can enhance photocatalytic activity (Zhang et al., 2016). The presence of hydroxyl groups plays a key role in enhancing photocatalytic activity as they act as the primary scavengers of photogenerated electrons and holes, leading to the formation of hydroxyl radicals (OH•) necessary for the degradation of RR4 dye. The anatase phase of TiO_2 is evident from the peaks in the range of 650-1400 cm^{-1}, indicating the lattice vibration of Ti-O-Ti stretching, which confirmed the presence of metal-oxygen bonding. The peaks at 1382 cm^{-1} corresponded to TiO_2-Ag, suggesting that Ag had been successfully deposited on the pores of the TiO_2 nanoparticles (Desiati et al., 2019; Govindan & Soliman, 2017). The peak observed at 2930 cm^{-1} corresponds to Ag_2O, representing the Ag-O vibration. Elyamny et al. (2021) stated that an absorption band at 653 cm^{-1} represents the Ag-O stretching mode, corresponding to the Ag-O vibration in Ag_2O. Therefore, this confirmed that TiO_2 was successfully doped with Ag_2O, and the formation of Ag is also evident, corroborating the previously mentioned XRD and FESEM-EDX results. Furthermore, upon observation, the main difference was found in the peak intensity of Ag_2O in the optimal 3 % $Ag_2O/Ag\text{-}TiO_2$ sample, which was the lowest compared to the other samples. This may be attributed to most of the silver precursor having been transformed into Ag^0. Fortunately, the presence of Ag^0 catalyses the heterojunction between $Ag/Ag_2O\text{-}TiO_2$, as the Ag metal in the system can absorb visible light due to surface plasmon resonance and also act as an electron trap to activate reaction sites.

PL analysis was also conducted to investigate the migration and separation of photogenerated electron-hole (e^-/h^+) pairs. A low intensity PL indicates a low recombination rate of photogenerated charge carriers, which can improve photocatalytic performance. As shown in Figure 6, all samples exhibited an emission peak in the range of 400-700 nm. In the case of pure unmodified TiO_2, the strong signal at 500 nm was associated with Wannier-Mott free excitation emission. The 3 % $Ag/Ag_2O\text{-}TiO_2$ sample exhibited a lower intensity signal compared to unmodified TiO_2. This can be explained by the p-n heterojunction between Ag_2O and TiO_2, which enhances charge transfer and suppresses the recombination of photogenerated e^-/h^+ pairs due to the synergistic effect. The presence of Ag^0, as proven by HRTEM, also contributes to this effect by acting as a conductive bridge for photogenerated charges, facilitating charge transfer and promoting the separation of photogenerated e^-/h^+ pairs in the system, thereby improving photocatalytic performance.

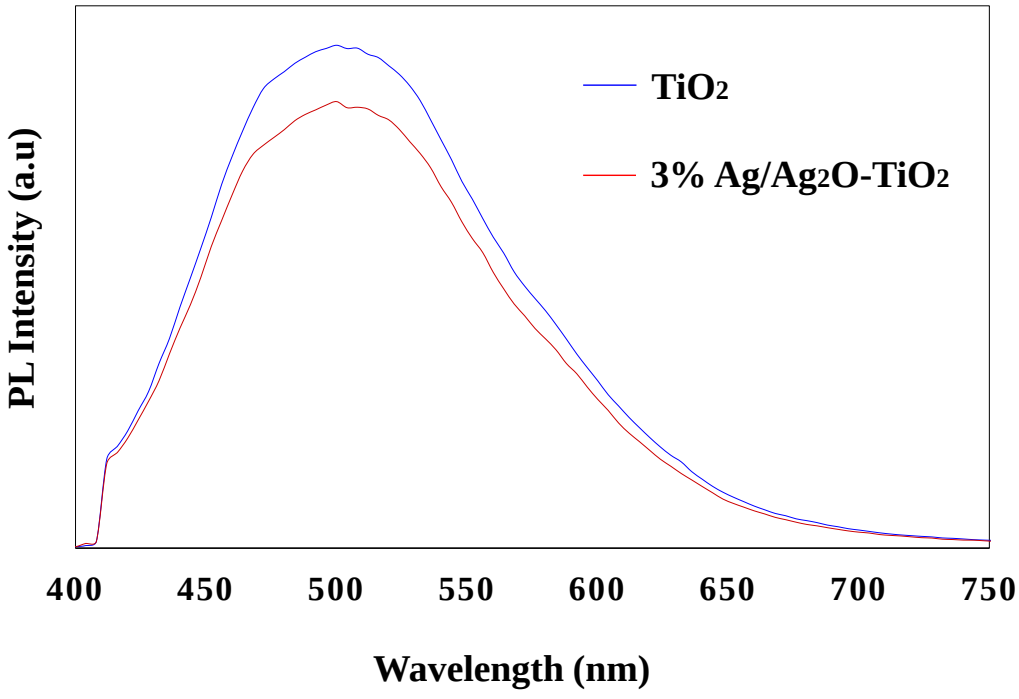

Figure 6. PL spectra for unmodified TiO_2 and modified of 3% $Ag/Ag_2O\text{-}TiO_2$.

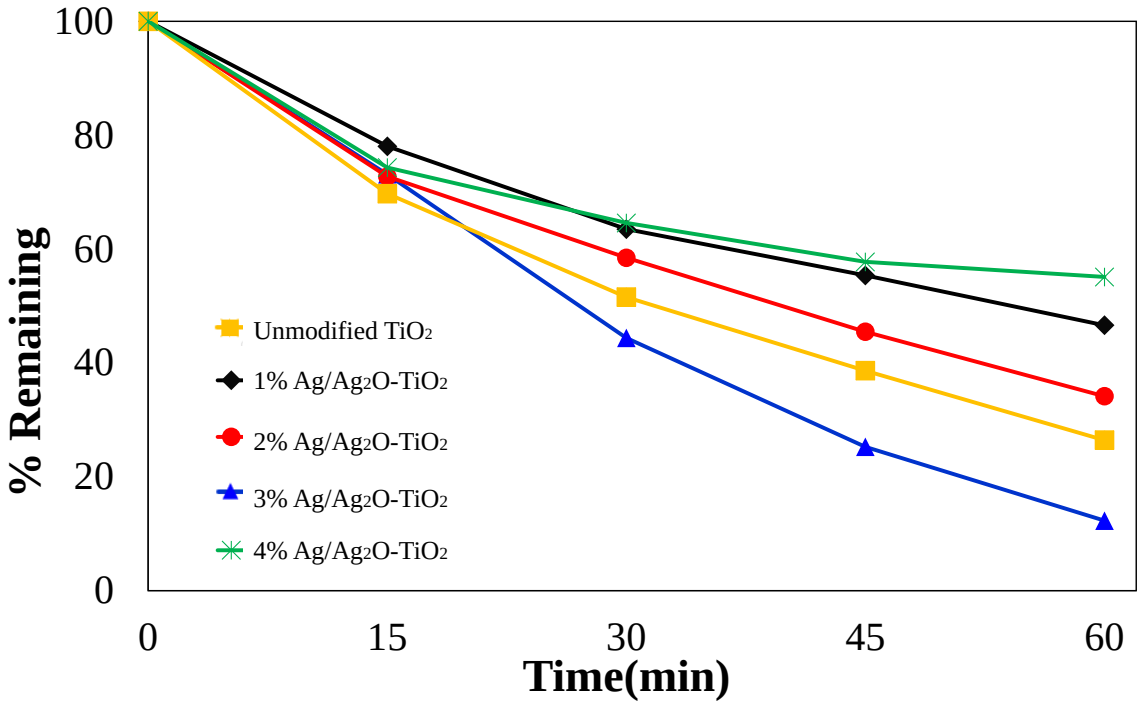

Figure 7. Percentage remaining of RR4 after photodegradation process for 60 mins

These mechanisms minimize the rate of e^-/h^+ recombination while increasing the ability of the photocatalysts to absorb visible light. The as-synthesised $Ag/Ag_2O\text{-}TiO_2$ nanoparticles have capabilities that make them perfect for use as photocatalysts. Furthermore, electrons trapped due to defects on the TiO_2 lattice can act as charge traps, impeding the movement of free electrons and reducing their availability for radiative processes. Limited electron mobility restricts their ability to recombine efficiently, resulting in a decrease in PL intensity. The trapped electrons and surface-bound holes can recombine, impacting the overall charge dynamics and the efficiency of charge utilization in photocatalytic processes (Komaraiah et al., 2020)

Photocatalytic Degradation study

The photocatalytic activity of the prepared photocatalysts was assessed using the photodegradation of RR4 dye under visible light by a reverse method. Figure 7 presents the percentage of RR4 dye remaining after the photocatalytic degradation of unmodified and modified Ag_2O-doped TiO_2, along with commercial P25 and $Ag/Ag_2O\text{-}TiO_2$ used as benchmarks. Based on Figure 7, after one hour of exposure to visible light, 1 % $Ag/Ag_2O\text{-}TiO_2$ and 4 % $Ag/Ag_2O\text{-}TiO_2$ exhibited similar photocatalytic activity, decolourising approximately 40 % of the RR4 dye. In contrast, unmodified TiO_2 and 2 % $Ag/Ag_2O\text{-}TiO_2$ demonstrated significantly higher photocatalytic performance with RR4 degradation rates of 70 % and 60 %, respectively. Interestingly, 3 % $Ag/Ag_2O\text{-}TiO_2$ showed the highest RR4 degradation performance among the studied samples, achieving more than 85 % decolourisation. Notably, all unmodified and modified Ag_2O and Ag-doped TiO_2 photocatalysts exhibited more than 40 % decolorization of RR4 dye within one hour of light irradiation. The adsorption and desorption of RR4 dye play a vital role in determining the efficiency of the photocatalyst. In the case of the 3 % $Ag/Ag_2O\text{-}TiO_2$, it was observed that RR4 began to adsorb on the surface of the immobilized photocatalyst particles when they were mixed with the RR4 solution. A previous study has reported that differences in particle surface area and electrical charge may be responsible for the adsorption mechanism between RR4 and 3 % $Ag/Ag_2O\text{-}TiO_2$ (Rahmawati et al., 2023). This can be attributed to the excess Ag and Ag_2O formed on the surface of the immobilized TiO_2 which creates positive charges, while RR4 dye carries negative electric charges. The strong electrostatic force between the dye and particle mixture leads to a significant decrease in RR4 concentration.

The Langmuir-Hinshelwood pseudo-first-order model was employed to calculate the kinetic rate constant (ka) for the photocatalytic reaction shown in Figure 8. This was done by analysing the linear fitting of ln (C_t/C_o) versus time, with an R^2 value above 0.85. The calculated kinetic rate constants are listed in Table 2 (Long et al., 2018). Among all the samples, 3 % $Ag/Ag_2O\text{-}TiO_2$ exhibited the highest RR4 degradation rate under visible light, with a rate constant of 3.21 x 10^{-2} h^{-1}. This indicated the fastest reaction rate. The increased photocatalytic activity of 3 % $Ag/Ag_2O\text{-}TiO_2$ can be attributed to factors such as its high surface area, strong dye adsorption capability, and an appropriate anatase-rutile ratio.

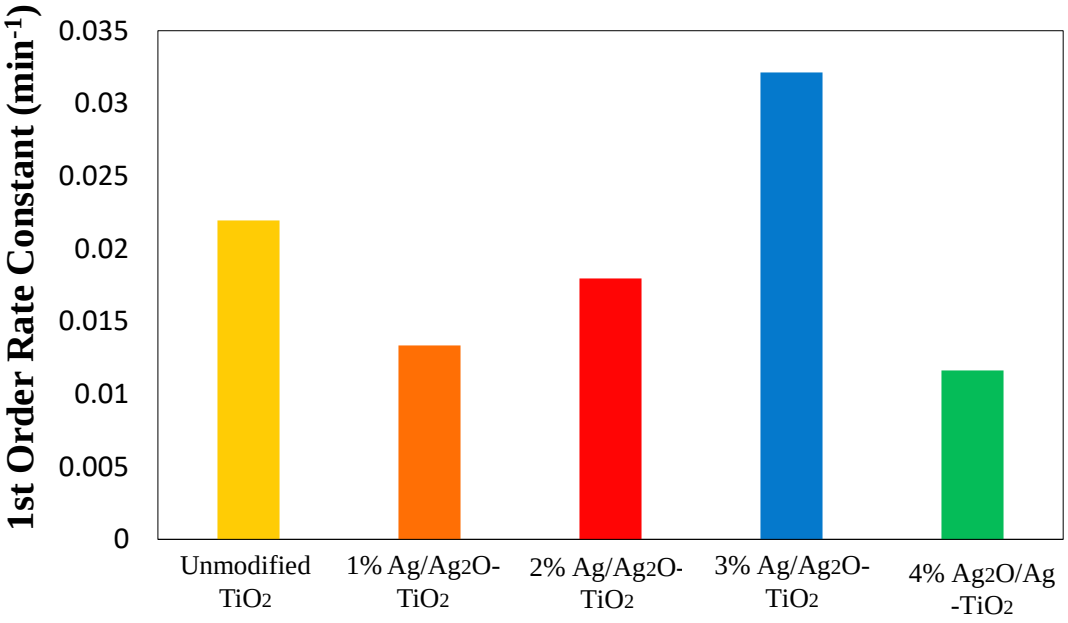

Figure 8. k-Value of photodegradation of RR4 Dyes.

Table 2. Kinetic rate constants for the photocatalysts.

Photocatalyst	Kinetic rate constant (x 10^{-2}) (h^{-1})
Unmodified TiO_2	2.19
1% Ag/Ag_2O-TiO_2	1.33
2% Ag/Ag_2O-TiO_2	1.79
3% Ag/Ag_2O-TiO_2	3.21
4% Ag/Ag_2O-TiO_2	1.16

The increase in efficiency of the prepared TiO_2 after being doped with Ag_2O using a silver precursor may be due to the incomplete conversion of the silver nitrate precursor into silver oxide. However, this phenomenon has had positive effects in the presence of silver. It is a good approach to enhance photocatalytic activity by altering the electronic structure of the composite material's Fermi level and preventing electron recombination. This effect can be attributed to surface plasmon resonance (SPR) or LSPR, which can enhance and modulate electromagnetic fields, light absorption and scattering (Sun et al., 2021). The presence of Ag_2O and Ag on the TiO_2 lattice can influence the photocatalytic oxidation reactions of the prepared Ag/Ag_2O-TiO_2 photocatalyst. Defects such as dislocations, vacancies, or impurity sites can occur due to the presence of Ag and Ag_2O on the TiO_2 lattice (Ode et al., 2023). These defects play a crucial role in enhancing the performance of TiO_2 as the main photocatalyst. They create localized energy levels within the band structure of TiO_2, resulting in additional electronic states. These states enhance the separation and transfer of charge carriers, reduce recombination, and increase the availability of reactive species for oxidation reactions (Zhao et al., 2017). Furthermore, the presence of Ag and Ag_2O induces oxygen vacancies in the lattice of TiO_2. These vacancies act as electron traps and facilitate the migration of photogenerated electrons to the TiO_2 surface, where they can participate in oxygen reactions. This confirms that the presence of Ag_2O and Ag has a significant impact on the performance of the TiO_2 photocatalyst. However, the agglomeration of Ag nanoparticles into larger clusters on the surface, which might restrict surface reaction sites and impede light absorption and adsorption of reactant molecules by TiO_2, could account for the decrease in photocatalytic activity observed in Ag/Ag_2O-TiO_2 samples with significant Ag decoration (e.g., 4% Ag_2O-TiO_2) (Mogal et al., 2014).

Table 3. Recent reports on $Ag/Ag_2O\text{-}TiO_2$.

Photocatalyst	Fabrication Technique	Substance Degraded	Photocatalytic Performance	Ref
Ag/TiO_2	Spin coated	Ethylene	Degradation of ethylene at 43.9-91.2%	(Thi et al., 2023)
Ag/TiO_2	Spin coated	Methyl orange (MO)& Methylene blue (MB)	Degradation of MB at 98.85% and MO at 96.34%	(Komaraiah et al., 2020)
Ag/TiO_2	Sol-gel	Oxytetracycline	Degradation > 94%	(Hieu et al., 2023)
Ag/TiO_2	Hydrothermal	MB dye	MB degradation > 94%	(Aravind et al., 2023)
Ag/TiO_2	Photoreduction	MB dye	MB degradation > 97.89%	(Lin et al., 2023)
Ag/TiO_2	In-situ reduction	Rhodamine (RhB) dye	RhB degradation > 97.8%	(Tian et al., 2023)
$Ag/Ag_2O\text{- }TiO_2$	Sol-gel	Imazaphyr herbicide	Total degradation 100% after 180 min	(Mkhalid et al., 2020)
Ag_2O/TiO_2	Wet precipitation	RhB dye	RhB degradation of 94.7%	(Gao & Wang, 2021)
$Ag\text{-}Ag_2O\text{-}TiO_2$	Magnetron sputtering	RhB dye	RhB degradation of 68.7%	(Yu et al., 2020)
Ag_2O/TiO_2	Facile wet chemical	RhB, MB dye, 4-nitrophenol	MB dye = 94%, RhB dye = 59%, 4-nitrophenol = 90.6%	(Mohapatra et al., 2020)
$Ag\text{-}Ag_2O\text{-}TiO_2$	Photodeposition	RhB dye	RhB dye degradation of 80%	(Vodyankin et al., 2021)

The low photocatalytic performance of the modified 1 %, 2 %, and 4 % $Ag/Ag_2O\text{-}TiO_2$ samples may be attributed to the reverse preparation method employed in this study. In the conventional method, $Ag_2O\text{-}TiO_2$ is prepared by doping Ag into a slurry form of TiO_2 powder prior to immobilization (Ismail et al., 2015). However, in the present study, a reverse method was used where the immobilized TiO_2 was prepared before the photodeposition of Ag_2O. This method may result in lower photocatalytic activity as there could be less contact between $Ag_2O\text{-}TiO_2$ and the dye due to the immobilization prior to photo-deposition. Table 3 provides an overview of various potential techniques for preparing $Ag/Ag_2O\text{-}TiO_2$ photocatalysts. The efficiency of the $Ag_2O\text{-}TiO_2$ photocatalyst prepared using the normal method has been reported to be low, possibly due to the limited contact between $Ag_2O\text{-}TiO_2$ and the dye. In this study, the reverse method was employed, where the immobilized TiO_2/DSAT was immersed in an aqueous solution of $AgNO_3$ in isopropyl alcohol (IPA) during photodeposition. This method was expected to enhance the photocatalytic activity of TiO_2 after doping with Ag_2O, as the particles were anticipated to be located within the outer layer pores or inside the TiO_2 pores, as shown in Figure 9 (a). The silver particles were expected to be distributed throughout the system due to the photodeposition method, as confirmed by the XRD and FTIR results. The presence of more $Ag/Ag_2O\text{-}TiO_2$ on the surface layer could increase the contact between $Ag/Ag_2O\text{-}TiO_2$ and the dye compared to a photocatalyst prepared by the normal method. Consequently, this may enhance the performance of $Ag/Ag_2O\text{-}TiO_2$ in degrading RR4 dyes. Fortunately, during the preparation process, a good heterojunction and Z-scheme heterojunction system were indirectly formed through the interaction facilitated by the excess Ag metal acting as an electron shuttle mediator in $Ag/Ag_2O\text{-}TiO_2$ (Sun et al., 2021; Fu et al., 2015). The Z-scheme system promotes the separation of electron-hole pairs and retains a prominent redox ability, as depicted in Figure 9 (b). Photoinduced electron transfer occurs to the metallic Ag^0 on the composite surface, which acts as an electron pool and

reduces the probability of electron-hole recombination. The trapped electrons on Ag^0 or the conduction band of TiO_2 can be transferred to oxygen on the nano-composite surface, leading to the generation of superoxide radicals (Zhou et al., 2019; Shume et al., 2020). The possible reaction steps involved in the photocatalytic degradation process of Ag_2O/Ag/TiO_2 are described in equation 3:

$$Ag_2O + hv \rightarrow Ag_2O\ (e^-_{CB} + h^+_{VB})$$

$$Ag_2O\ (e^-) + Ag \rightarrow Ag\ (e^-) \rightarrow TiO_2\ (e^-)$$

$$TiO_2\ (e^-) + O_2 \rightarrow TiO_2 + O_2{\bullet}^-$$

$$O_2{\bullet}^- + H_2O \rightarrow HO_2{\bullet} + {}^-OH \quad (3)$$

$$2HO_2{\bullet} \rightarrow H_2O_2 + O_2$$

$$H_2O_2 + e^- \rightarrow {\bullet}OH + {}^-OH$$

$${\bullet}OH\ /O_2^- + \text{RR4 dyes} \rightarrow \text{degradation product}$$

CONCLUSION

A Ag/Ag_2O-TiO_2 photocatalyst was successfully modified using a reverse method. Characterization by FTIR, FESEM-EDX and XRD confirmed that Ag_2O was successfully doped onto the TiO_2 surface. The presence of excess Ag metal in the system created a Z-scheme heterojunction system that helped to boost photocatalytic performance. In comparison to undoped immobilized TiO_2, the photodegradation of RR4 under immobilized Ag/Ag_2O-TiO_2 significantly increased with 3 % loading.

ACKNOWLEDGEMENTS

We would like to acknowledge Universiti Teknologi MARA (UiTM) for providing all the facilities. This work also was supported by Ministry of Higher Education (MOHE) under Fundamental Research Grant Scheme: FRGS/1/2022/STG04/ UITM/02/1.

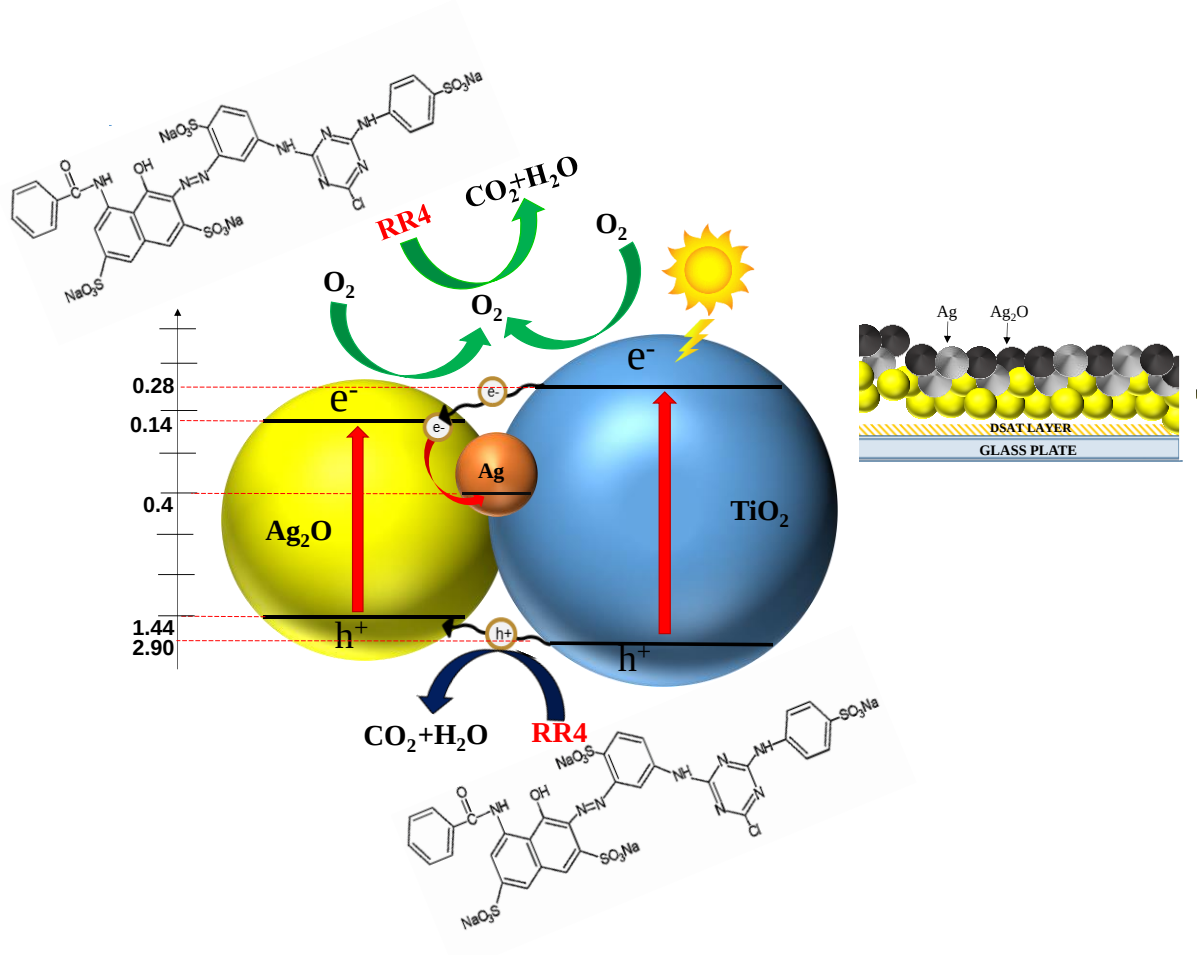

Figure 9. (a) Expected dispersion of Ag and Ag_2O particles on TiO_2/DSAT (b) Proposed mechanism Z-scheme heterojunction effect of Ag/Ag_2O-TiO_2.

REFERENCES

1. Ain, S. K., Azami, M. S., Zaharudin, R., Bakar, F. & Nawawi, W. I. (2016) Photocatalytic Study of New Immobilized TiO_2 Technique towards Degradation of Reactive Red 4 Dye. *MATEC Web of Conferences*, **47**, 05019.

2. Albero, J. & García, H. (2019) Catalysis by supported gold nanoparticles. In *Comprehensive Nanoscience and Nanotechnology, Elsevier*, **1–5**, 91–108.

3. Alsheheri, S. Z. (2021) Nanocomposites containing titanium dioxide for environmental remediation. *Designed Monomers and Polymers*, **24(1)**, 22–45.

4. Aravind, M., Amalanathan, M., Aslam, S., Noor, A. E., Jini, D., Majeed, S., Velusamy, P., Alothman, A. A., Alshgari, R. A., Sheikh, M. & Mushab, S. (2023) *Chemosphere Hydrothermally synthesized Ag-TiO_2 nanofibers (NFs) for photocatalytic dye degradation and antibacterial activity*, **321**, January.

5. Arekhi, M. & Jamshidi, M. (2018) Progress in Organic Coatings Influences of inorganic binder on photocatalytic oxidation (PCO) and degradation of nano/micro TiO_2 containing acrylic composites. *Progress in Organic Coatings*, **115**, 1–8, January 2017.

6. Azami, M. S., Ismail, K., Ishak, M. A. M., Zuliahani, A., Hamzah, S. R. & Nawawi, W. I. (2020) Journal of Water Process Engineering Formation of an amorphous carbon nitride/ titania composite for photocatalytic degradation of RR4 dye. *Journal of Water Process Engineering*, **35**, 101209, February.

7. Azami, M. S., Nawawi, W. I., Jawad, A. H., Ishak, M. A. M. & Ismail, K. (2017) Ndoped TiO_2 Synthesised via Microwave Induced Photocatalytic on RR4 Dye Removal under LED Light Irradiation. **46(8)**, 1309–1316.

8. Bakar, F., Azami, M. S., Ain, S. K., Zaharudin, R. & Nawawi, W. I. (2016) A Study on RR4 Dye as a Sensitizer in Enhancing Photoactivity of Immobilized Photocatalysts. July.

9. Basavarajappa, P. S., Patil, S. B., Ganganagappa, N., Reddy, K. R., Raghu, A. V. & Reddy, C. V. (2020) Recent progress in metal-doped TiO_2, non-metal doped/codoped TiO_2 and TiO_2 nano-structured hybrids for enhanced photocatalysis. *International Journal of Hydrogen Energy*, **45(13)**, 7764– 7778.

10. Binitha, N., Yaakob, Z., Reshmi, M., Sugunan, S., Ambili, V. & Zetty, A. (2009) Preparation and characterization of nano silver-doped mesoporous titania photocatalysts for dye degradation. *Catalysis Today*, **147**, S76–S80.

11. Chaturvedi, R. & Singh, P. K. (2021) Synthesis and characterization of nano crystalline nitrogen doped titanium dioxide. *Materials Today: Proceedings*, **45**, 3666–3669.

12. Corma, A. & Garcia, H. (2008) Supported gold nanoparticles as catalysts for organic reactions. In *Chemical Society Reviews*, **9**, 1-10.

13. Desiati, R. D., Taspika, M. & Sugiarti, E. (2019) Effect of calcination temperature on the anti-bacterial activity of TiO_2/Ag nanocomposite. *Effect of calcination temperature on the antibacterial activity of TiO_2/Ag nanocomposite Manuscript version: Accepted Manuscript*, April.

14. Elyamny, S., Eltarahony, M., Abu-Serie, M., Nabil, M. M. & Kashyout, A. E.-H. B. (2021) One-pot fabrication of Ag@Ag_2O core–shell nanostructures for biosafe antimicrobial and antibiofilm applications. *Scientific Reports*, **11(1)**, 1–14.

15. Estephane, G. C. & El Jamal, M. M. (2019) Effect of doping of TiO_2 nanoparticles with silver on their photocatalytic activities toward degradation of E 131 VF. *Journal of Chemical Technology and Metallurgy*, **54(5)**, 926–933.

16. Fu, J., Cao, S. & Yu, J. (2015) Dual Z-scheme charge transfer in TiO_2–Ag–Cu_2O composite for enhanced photocatalytic hydrogen generation. *Journal of Materiomics*, **1(2)**, 124–133.

17. Gao, Y. & Wang, T. (2021) Preparation of Ag_2O/ TiO_2 nanocomposites by two-step method and study of its degradation of RhB. **1224**.

18. Gilja, V., Kratofil Krehula, L., Katančić, Z., Krehula, S., Hrnjak-Murgić, Z. & Travas Sejdic, J. (2018) Influence of Titanium Dioxide Preparation Method on Photocatalytic Degradation of Organic Dyes. *Croatica Chemica Acta*, **91(3)**, 323 – 335.

19. Gomes, J. F., Lopes, A., Bednarczyk, K., Gmurek, M., Stelmachowski, M., Zaleska Medynska, A., Quinta-Ferreira, M. E., Costa, R., Quinta-Ferreira, R. M. & Martins, R. C. (2018) Effect of noble metals (Ag, pd, pt) loading over the efficiency of TiO_2 during photocatalytic ozonation on the toxicity of parabens. *Chem Engineering*, **2(1)**, 1–14.

20. González-torres, J. C., Poulain, E., Domínguez-soria, V., García-cruz, R. & Olveraneria, O. (2018) *Vacancies: Photocatalysts Active in the Visible Region*, 1–12.

21. Govindan, B. & Soliman, A. R. (2017) Sol-Gel-Assisted Microwave-Derived Synthesis of Anatase

Ag / TiO_2 / GO Nanohybrids toward Efficient Visible Light Phenol Degradation. May.

22. Heo, N., Jun, Y. & Park, J. H. (2013) Dye molecules in electrolytes: new approach for suppression of dye-desorption in dye-sensitized solar cells. 1–6.

23. Hieu, C., Tuong, T., Tran, V., Lien, M. & Juang, R. (2023) Journal of the Taiwan Institute of Chemical Engineers Facile synthesis of reusable Ag / TiO_2 composites for efficient removal of antibiotic oxytetracycline under UV and solar light irradiation. **145**, December 2022.

24. Hoffmann, S., Pablo, J., Werner, F., Moreno-villoslada, I. & Goycoolea, F. M. (2016) Conference paper new insights into the nature of the Cibacron brilliant red 3B-A – Chitosan interaction. **88(9)**, 891– 904.

25. Hoşgün, H. L. & Aydın, M. T. A. (2019) Synthesis, characterization and photocatalytic activity of boron doped titanium dioxide nanotubes. *Journal of Molecular Structure*, **1180**, 676–682.

26. Ismail, I., Nawawi, W. I. & Nawi, M. A. (2014) Preparation of a thin carbon coated TiO_2 using humic acid for the enhanced removal of reactive red 4 dye. *Reac Kinet Mech Cat*, **114**, 323–339.

27. Jin, Z., Duan, W., Duan, W., Liu, B., Chen, X., Yang, F. & Guo, J. (2016) Indium doped and carbon modified P25 nanocomposites with high visible light sensitivity for the photocatalytic degradation of organic dyes. **517**, 129–140.

28. Khan, M. M., Adil, S. F. & Al-Mayouf, A. (2015) Metal oxides as photocatalysts. 462–464.

29. Khan, M. A. M., Kumar, S., Ahmed, J. & Ahamed, M. (2021) Influence of silver doping on the structure, optical and photocatalytic properties of Ag-doped $BaTiO_3$ ceramics. *Materials Chemistry and Physics*, **259**, 124058, (November 2020).

30. Khang, N. C., Van, D. Q., Thuy, N. M., Minh, N. Van & Minh, P. N. (2016) Remarkably enhanced photocatalytic activity by sulfur-doped titanium dioxide in nanohybrids with carbon nanotubes. *Journal of Physics and Chemistry of Solids*, **99**, 119–123.

31. Kishor, R., Purchase, D., Saratale, G. D., Ferreira, L. F. R., Bilal, M., Iqbal, H. M. N. & Bharagava, R. N. (2021) Environment friendly degradation and detoxification of Congo red dye and textile industry wastewater by a newly isolated Bacillus cohnni (RKS9). *Environmental Technology and Innovation*, **22**, 101425.

32. Komaraiah, D., Radha, E., Sivakumar, J., Reddy, M. V. R. & Sayanna, R. (2020) Photoluminescence and photocatalytic activity of spin coated Ag^+ doped anatase TiO_2 thin films. *Optical Materials*, **108**, 110401, (June).

33. Kouhail, M., Elberouhi, K., Elahmadi, Z., Benayada, A. & Gmouh, S. (2020) A Comparative study between TiO_2 and ZnO photocatalysis: Photocatalytic degradation of textile dye. *IOP Conference Series: Materials Science and Engineering*, **827**, 012009.

34. Lin, Q., Zhu, Y., Wang, Q., Huang, Y. & Zhou, Z. (2023) A facile and new preparation of crystalline Ag loaded TiO_2 nanoparticles by a one-step method at room temperature. **164**, March.

35. Liao, C., Li, Y. & Tjong, S. C. (2020) Visible-Light Active Titanium Dioxide Nanomaterials with Bactericidal Properties. *Nanomaterials*, **10(1)**, 124.

36. Long, G., Ding, J., Xie, L., Sun, R., Chen, M., Zhou, Y., Huang, X., Han, G., Li, Y. & Zhao, W. (2018) Fabrication of mediator-free g-C_3N_4/Bi_2WO_6 Z-scheme with enhanced photocatalytic reduction dechlorination performance of 2,4-DCP. *Applied Surface Science*, **455**, 1010–1018, April.

37. Mkhalid, I. A., Fierro, J. L. G., Mohamed, R. M. & Alshahri, A. A. (2020) Visible light driven photooxidation of imazapyr herbicide over highly efficient mesoporous Ag / Ag_2O–TiO_2 p-n heterojunction photocatalysts. **46**, 25822–25832, May.

38. Mogal, S. I., Gandhi, V. G., Mishra, M., Tripathi, S., Shripathi, T., Joshi, P. A. & Shah, D. O. (2014) Single-Step Synthesis of Silver-Doped Titanium Dioxide: Influence of Silver on Structural, Textural, and Photocatalytic Properties. *Industrial & Engineering Chemistry Research*, **53(14)**, 5749–5758.

39. Moma, J. & Baloyi, J. (2018) Modified Titanium Dioxide for Photocatalytic Applications. In *Intech*, **32**, 137–144, July.

40. Mohapatra, S., Singh, J. & Satpati, B. (2020) Journal of Physics and Chemistry of Solids Facile synthesis, structural, optical and photocatalytic properties of mesoporous Ag_2O / TiO_2 nano-heterojunctions. **13**.

41. Nasikhudin, Diantoro, M., Kusumaatmaja, A. & Triyana, K. (2018) Study on Photocatalytic Properties of TiO_2 Nanoparticle in various pH condition. *Journal of Physics: ConferenceSeries*, **1011(1)**.

42. Nawi, M. A. & Nawawi, I. (2013) Preparation and characterization of TiO_2 coated with a thin carbon layer for enhanced photocatalytic activity under fluorescent lamp and solar light irradiations. **453**, 80–91.

43. Nawi, M. A. & Sabar, S. (2012) Journal of Colloid and Interface Science Photocatalytic decolourisation of Reactive Red 4 dye by an immobilised TiO_2 / chitosan layer by layer system. *Journal of Colloid and Interface Science*, **372(1)**, 80–87.

44. Ode, L., Salim, A., Zakir, M., Zaeni, A., Maulidiyah, M., Nurdin, M., Naqiyah, S., Ridwan, J. & Ali, A. (2023) Journal of Physics and Chemistry of Solids Improved photoactivity of TiO_2 photoanode of dye-sensitized solar cells by sulfur doping. **175**, January.

45. Ohtani, B., Guskos, N. & Morawski, A. W. (2015) Applied Catalysis B: Environmental Nitrogen-doped, metal-modified rutile titanium dioxide as photocatalysts for water remediation. **162**, 310–318.

46. Oje, A. I., Ogwu, A. A. & Oje, A. M. (2021) Effect of temperature on the electrochemical performance of silver oxide thin fi lms super-capacitor. **882**, 1–6.

47. Ong, T. C., Verel, R. & Copéret, C. (2016) Solid-state NMR: Surface chemistry applications. In *Encyclopedia of Spectroscopy and Spectrometry*, *Elsevier*, 121–127.

48. Ortega-Liébana, M. C., Sánchez-López, E., Hidalgo-Carrillo, J., Marinas, A., Marinas, J. M. & Urbano, F. J. (2012) A comparative study of photocatalytic degradation of 3chloropyridine under UV and solar light by homogeneous (photo-Fenton) and heterogeneous (TiO_2) photocatalysis. *Applied Catalysis B: Environmental*, **127**, 316–322.

49. Paul, D. R., Sharma, R., Panchal, P., Nehra, S. P., Gupta, A. P. & Sharma, A. (2020) Synthesis, characterization and application of silver doped graphitic carbon nitride as photocatalyst towards visible light photocatalytic hydrogen evolution. *International Journal of Hydrogen Energy*, **45(44)**, 23937–23946.

50. Qian, R., Zong, H., Schneider, J., Zhou, G., Zhao, T., Li, Y., Yang, J., Bahnemann, D. W. & Pan, J. H. (2019) Charge carrier trapping, recombination and transfer during TiO_2 photocatalysis: An overview. *Catalysis Today*, **335**, 78–90.

51. Ramos, R., Scoca, D., Borges Merlo, R., Chagas Marques, F., Alvarez, F. & Zagonel, L. F. (2018) Study of nitrogen ion doping of titanium dioxide films. *Applied Surface Science*, **443**, 619–627.

52. Razak, S., Nawi, M. & Haitham, K. (2014) Fabrication, characterization and application of a reusable immobilized TiO2–PANI photocatalyst plate for the removal of reactive red 4 dye. *Applied Surface Science*, **319**, 90–98.

53. Rozina, Ahmad, M., Asif, S., Sultana, S., Mukhtar, A., Zafar, M., Ahmed, A., Ullah, S., Shariq, M., Krishna, A., Mofijur, M. & Show, P. (2022) Conversion of the toxic and hazardous Zantho-xylum armatum seed oil into methyl ester using green and recyclable silver oxide nanoparticles. **310**, June 2021.

54. Sarteep, Z., Pirbazari, A. E. & Aroon, M. A. (2016) Silver Doped TiO_2 Nanoparticles: Preparation, Characterization and Efficient Degradation of 2, 4dichlorophenol Under Visible Light**. 1(2)**, 135–144.

55. Schneider, J., Matsuoka, M., Takeuchi, M., Zhang, J., Horiuchi, Y., Anpo, M. & Bahnemann, D. W. (2014) Understanding TiO_2 Photocatalysis: Mechanisms and Materials. *Chemical Reviews*, **114(19)**, 9919–9986.

56. Shume, W. M., Murthy, H. C. A. & Zereffa, E. A. (2020) A Review on Synthesis and Characterization of Ag_2O Nanoparticles for Photocatalytic Applications.

57. Singh, S., Singh, P. K. & Mahalingam, H. (2014) Novel Floating Ag^+-Doped TiO_2/Polystyrene Photo-catalysts for the Treatment of Dye Wastewater. *Industrial & Engineering Chemistry Research*, **53(42)**, 16332–16340.

58. Sulaiman, S. N. A., Zaky Noh, M., Nadia Adnan, N., Bidin, N. & Ab Razak, S. N. (2018) Effects of photocatalytic activity of metal and non-metal doped TiO_2 for Hydrogen production enhancement - A Review. *Journal of Physics: Conference Series*, **1027(1)**.

59. Sun, Q., Hou, P., Wu, S., Yu, L. & Dong, L. (2021) The enhanced photocatalytic activity of Ag-Fe_2O_3-TiO_2 performed in Z-scheme route associated with localized surface plasmon resonance effect. *Colloids and Surfaces A: Physico-chemical and Engineering Aspects*, **628**, July.

60. Tahir, M. B., Iqbal, T., Rafique, M., Rafique, M. S., Nawaz, T. & Sagir, M. (2020) Nanomaterials for photocatalysis. In *Nanotechnology and Photo-catalysis for Environmental Applications*, *Elsevier*, 65–76.

61. Tao, Wang & Xiao, Huan & Gao, Yang & Xu,

Jiahui & Zhang, Zhengmei & Bian, Haiqin & Sun, Tianyi. (2020). Ag_2O/TiO_2 hollow microsphere heterostructures with exposed high-energy {001} crystal facets and high photocatalytic activities. *Journal of Materials Science: Materials in Electronics*, 31.10.1007/s10854-020-03697-w.

62. Thi, P., Hoai, T., Dai, T., Thi, N., Huong, M., Thi, M. & Anh, V. (2023) Chemosphere Removal of ethylene by synthesized Ag/TiO_2 photocatalyst under visible light irradiation. **329**, 3–10, January.

63. Tian, Z., Song, Y., Tao, K., Liu, N., Qin, S., Yang, J., Li, J. & Cui, Z. (2023) Applied Surface Science Preparation of TiO_2-Ag heterostructure via tannic acid-assistance and its immobilization on PVDF membrane for the degradation of dye under visible light. **625**, January.

64. Varma, K. S., Tayade, R. J., Shah, K. J., Joshi, P. A., Shukla, A. D. & Gandhi, V. G. (2020) Photocatalytic degradation of pharmaceutical and pesticide compounds (PPCs) using doped TiO_2 nanomaterials: A review. *Water-Energy Nexus*, **3**, 46–61.

65. Viswanathan, B. (2018) Photocatalytic Degradation of Dyes: An Overview Photocatalytic Degradation of Dyes: An Overview. September.

66. Vodyankin, A. A., Belik, Y. A., Zaikovskii, V. I. & Vodyankina, O. V. (2021) Journal of Photochemistry & Photobiology, A: Chemistry Investigating the influence of silver state on electronic properties of $Ag/Ag_2O/TiO_2$ heterojunctions prepared by photodeposition. **408**, December 2020.

67. Waly, G. H. (2018) Effect of incorporating undoped or silver-doped photocatalytic titanium dioxide on the antifungal effect and dynamic viscoelastic properties of long-term acrylic denture liners. *Future Dental Journal*, **4(1)**, 8–15.

68. Wan Ismail, W. I. N., Ain, S. K., Zaharudin, R., Jawad, A. H., Ishak, M. A. M., Ismail, K. & Sahid, S. (2015) New TiO_2/DSAT Immobilization System for Photodegradation of Anionic and Cationic Dyes. *International Journal of Photoenergy*, 1–6.

69. Yu, H., Wu, Q., Wang, J., Liu, L., Zheng, B., Zhang, C., Shen, Y., Huang, C., Zhou, B. & Jia, J. (2020) Applied Surface Science Simple fabrication of the Ag-Ag_2O-TiO_2 photocatalyst thin films on polyester fabrics by magnetron sputtering and its photocatalytic activity. **503**, August 2019.

70. Zhang, Z., Chen, Y., Weng, J. & Hong, H. (2016) The analysis of TiO_2 doping by different ferric salts. *Ifeesd*, 512–516.

71. Zhao, H., Pan, F. & Li, Y. (2017) A review on the effects of TiO_2 surface point defects on CO_2 photoreduction with H_2O_3.

72. Zhou, H., Wen, Z., Liu, J., Ke, J., Duan, X. & Wang, S. (2019) Z-scheme plasmonic Ag decorated WO_3/Bi_2WO_6 hybrids for enhanced photocatalytic abatement of chlorinated-VOCs under solar light irradiation. *Applied Catalysis B: Environmental*, **242**), 76–84, October 2018.